Riset Geologi dan Pertambangan
Earth science journal · Open access · BRIN Earth Sciences & Maritime · BRIN Publishing
ISSN 0125-9849 e-ISSN 2354 6638

RESEARCH ARTICLE
OPEN ACCESS

Riset Geologi dan Pertambangan (2026) Vol. 36, No. 1, 1–12
DOI: 10.55981/risetgeotam.2026.1374

Keywords:
Galungung volcano
sector collapse
gravity
subsurface fault
The Thousand Hills of Tasikmalaya

Corresponding author:
Muhammad Naufaldi
mnaufaldi1@gmail.com

Article history:
Received: 27 March 2025
Revised: 03 December 2025
Accepted: 12 December 2025

Author Contributions:
Conceptualization: MN, IA, S, HG
Data curation: YS,
Formal analysis: MN, IH, IA, and S
Investigation: MN, IA, YS,
Methodology: MN, IH, IA, S, HG
Supervision: IA, S, MAM, HG
Visualization: MN, IH, and IA
Writing–original draft: MN, IA, S
Writing–review & editing: MN, IH, S, MAM, HG

Citation:
Naufaldi, M., Hamida, I., Arisbaya, I., Sudrajat, Y., Sungkono, S., Masinai, M.A., Grandis, H., 2026. Gravity analysis of a subsurface fault controlling the sector collapse of Galunggung Caldera, Indonesia. J. Ris. Geol. Pertamb., 36 (1), 1–12, doi: 10.55981/risetgeotam.2026.1374

Gravity analysis of a subsurface fault controlling the sector collapse of Galunggung Caldera, Indonesia

Muhammad Naufaldi[1], Izzuki Hamida[2,3], Ilham Arisbaya[2], Yayat Sudrajat[2], S. Sungkono[1], M. Altin Masinai[4], Hendra Grandis[3]

[1]Department of Physics, Institut Teknologi Sepuluh Nopember (ITS), Surabaya, Indonesia
[2]Research Center for Geological Disaster, National Research and Innovation Agency (BRIN), Bandung, Indonesia
[3] Faculty of Mining and Petroleum Engineering, Institut Teknologi Bandung (ITB), Bandung, Indonesia
[4] Faculty of Mathematics and Natural Science, Hasanuddin University (UNHAS), Makassar, Indonesia

Abstract

Galunggung volcano (7°15′S, 108°3′E) in West Java, Indonesia, is an active stratovolcano with a significant history of eruptions and widespread impacts on the surrounding area. One major eruption occurred around 4,200 years ago, causing a sector collapse in the southeastern part of the mountain and forming a caldera that shaped the landscape known as the Thousand Hills of Tasikmalaya. Previous studies explained the cause of this collapse as triggered by a massive eruption or by the steep-slope control to the southeast. However, both suggest a tectonic role that may have contributed to the flank collapse. The distribution of hot springs around Galunggung, which forms a lineament toward the caldera, may provide a clue regarding the factors controlling the sector collapse event. We analyzed 117 legacy gravity measurements collected in 2000 and reprocessed them using advanced techniques to examine the subsurface structure and investigate the possibility of a subsurface weak zone. Bouguer anomaly separation using a Butterworth Band-pass Filter and derivative analysis (FHD, FVD, TDX) revealed a linear NW-SE trending low-gravity anomaly (32.5–39.4 mGal) extending ~6 km southeast of Galunggung, indicating the presence of a subsurface fault. This interpretation is supported by the alignment of the distribution of geothermal manifestations and the orientation of the caldera's morphology, which opens in the same direction. This NW-SE inherited fault structure is interpreted to have played a dual role in the volcano dynamics, serving both as a pathway for the migration of hot fluid, which may decrease rock strength, and as a structural weakness intruded by magma. Thus, we propose that this pre-existing fault was a controlling factor in the collapse of Galunggung through a fault-parallel breaching mechanism. These findings have important implications for volcanic hazard assessment in densely populated areas around Galunggung.

1. Introduction

Galunggung is a stratovolcano located in West Java, Indonesia, recognized as an active volcano with a history of significant eruptions and widespread impacts on the surrounding area. At least four eruptions have been recorded throughout history, in 1822, 1894, 1918, and most recently in 1982-1983 (Bronto, 1989). One of the major eruptions known to have occurred ~4.2 ka, causing the sector collapse of the southeastern part of the mountain, produced a rock unit known as the Tasikmalaya Formation. This collapse resulted in significant morphological changes, creating an iconic landscape known as the Thousand Hills of Tasikmalaya (THT)(Bronto, 1989). THT is a debris avalanche product that has attracted the attention of scientists since the 1800s, from Junghuhn to Verbeek and Fenema (Siebert and Roverato, 2021). Various hypotheses were proposed to explain the origin of hummocky hills before Furuya (1978) identified a resemblance to the landform at Mt. Bandai in 1888 and Mt. Unzen in 1792. The THT spans approximately 32 square km west of Tasikmalaya city, and the hummocky hills are spread between 0.5 and 20 km from the summit of Galunggung (Alfin et al., 2022) (see Figure 1).

The formation of the THT is believed to be linked to the evolution of Galunggung around 4,200 BP (Bronto, 1989). Since the Old Galunggung cryptodome blocked the existing Guntur vent ~5.0 ka, the magma conduit shifted southeastward, and a new vent was developed on the southeast flank of Galunggung. The regional tectonic setting presumably controlled the shifting of the magma pathway (Bronto, 1989). Another opinion was presented by Marliyani et al. (2020), who analyzed crater morphology in Java to estimate the feeding orientation of the dikes and identify the principal stresses during dike emplacement. They identified faults around the Galunggung crater that align with the extension of the Telaga Bodas, located north of Galunggung, and interpreted the dike follow the pattern of an existing structure. The authors concluded that the direction of the breach at Galunggung differed from the crater elongation and the coeval cone elongation, indicating that another factor influenced the breach orientation.

These opinions suggest that the regional tectonic setting plays a crucial role in studying the volcanic collapse. Hot springs around the crater of Galunggung tend to occur in a straight line in the NW-SE direction, (Bronto, 1989; Budhitrisna, 2010; Martakusumah et al., 2015). This implies the existence of a subsurface fault that could affect the volcano-tectonic interaction in Galunggung. However, the distribution of the hot springs appears to be limited to the area around the crater, extending for about 3 km. However, no geophysical investigation has been conducted to verify this structural control. Here, we utilized gravity data to map the subsurface of the area around Galunggung, thereby identifying the factors that contributed to the sector collapse. The gravity method has been widely used in studying faults (e.g. Amir et al., 2021; Wu and Gao, 2019), particularly in inferring fault when the surface trace is hardly identified, for example, in volcanic areas (Arisbaya et al., 2024) Horizontal and vertical derivative analysis of Bouguer anomalies is useful for delineating the continuity of faults when part of them is covered by young sediments, as demonstrated in the Niigata Plain, Japan (Wada et al., 2017). In addition, normalized total horizontal derivative analysis can enhance the fainter anomaly discontinuities in the case of multi-object systems (Cooper and Cowan, 2006). The specific objectives are: (1) to identify subsurface fault structures using gravity analysis, (2) to determine the spatial relationship between faults and geothermal manifestations, and (3) to evaluate the role of pre-existing faults in the sector collapse mechanism.

2. Geological Setting

Galunggung volcano is located in West Java, with coordinates 7°15′S, 108°3′E. The crater of Galunggung is approximately 1 km in diameter and over 100 meters deep, known as the Guntur crater. However, the most prominent morphology of Galunggung is the horseshoe-shaped caldera, with a southeast-opening geometry approximately 9 km long and 3 to 6 km wide. Galunggung is part of the Sunda-Banda volcanic arc, which formed as the Indo-Australian Plate subducted beneath the Eurasian Plate. Tectonic activity in this zone generates heat sources that trigger volcanic activity in West Java, including Galunggung (Suryo and Clarke, 1985). The volcanic arc is situated in the middle of Java Island, so the Quaternary volcanoes appear to be located between Tertiary sedimentary rocks that crop out to the south and north of the arc (Budhitrisna, 2010).

The geology of Galunggung is often associated with Telaga Bodas, located ~3 km north of Galunggung caldera (see Figure 1). The Karaha–Telaga Bodas geothermal field is situated within a north-south trending volcanic ridge system, with Galunggung considered the youngest (Arisbaya et al., 2018; Nemčok et al., 2007). In fact, the collapse of Galunggung was hypothesized to be the trigger that transformed the Karaha–Telaga Bodas geothermal system from a high-temperature fluid-dominated system to a steam-dominated one (Moore et al., 2002). A recent study on the geochemical characteristics of volcanic rocks estimated that the subduction zone is shifting northward, from Galunggung to Karaha-Telaga Bodas (Al Kausar et al., 2024).

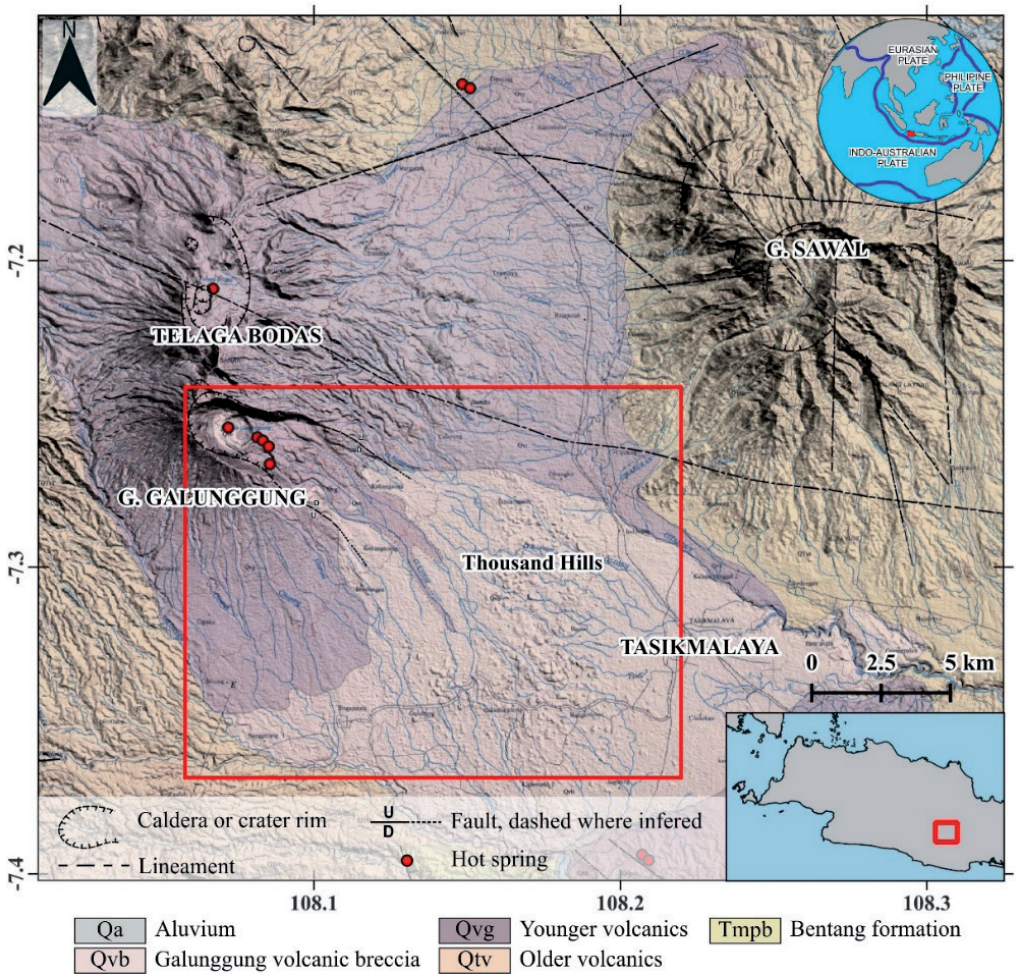

Figure 1. Geological map of Galunggung volcano and surroundings (after Budhitrisna, 2010). Hot springs from Budhitrisna (2010) and Martakusumah et al. (2015) show NW-SE alignment (dashed black line). The Red rectangle indicates the gravity survey area. Coordinates in UTM Zone 49S.

The geological map of the Galunggung volcano and its surrounding area (after Budhitrisna, 2010) indicates that most of the material in the Galunggung area consists of Quaternary volcanic breccia, comprising lava flows, pyroclastic deposits, dikes, cryptodomes, and lahars. These rocks represent the accumulation of eruption products from various periods of Galunggung's volcanic activity. The Tertiary Bentang Formation crops out in the south of Galunggung, and the structural pattern shows a southeastward trend parallel to the horseshoe caldera. The presence of the Cipanas, Cikunir, and Cibanjaran springs to the east and southeast is also thought to be controlled by subsurface fractures or faults (Bronto, 1989).

Galunggung has a long history of eruptions. Bronto (1989) explains that the eruption and formation of the area around Galunggung can be divided into three periods: the Old Galunggung Formation, Tasikmalaya Formation, and Cibanjar Formation. Material from the Old Galunggung Formation is associated with the Guntur crater, and volcanic activity is estimated to have occurred between 50,000 and 10,000 years ago. It consists of lava flows, pyroclastic flows, dikes, cryptodomes, and lahar deposits. The Tasikmalaya Formation is

associated with a major eruption approximately 4,200 ± 150 years ago. The Old Galunggung cryptodome plugged the pre-existing crater, and a new vent formed on the volcano's southeastern flank. The southeast part of Old Galunggung collapsed and slid down, creating the Thousand Hills of Tasikmalaya. Its rocks consist of volcanic debris avalanche deposits (DAD), pyroclastic flows, and lahar deposits. Meanwhile, Cibanjar Formation consists of pyroclastic flows, pyroclastic falls, and lahar deposits that formed from the 1822 eruption to the 1983 eruption.

3. Materials and Methods

3.1 Gravity Data Reprocessing

We reprocessed legacy gravity data acquired in 2000 by the LIPI-Japan collaborative survey using recent advanced techniques. This reprocessing provides higher resolution subsurface imaging than previous analyses (Nishida et al., 2001; Martakusumah et al., 2015). The study area is located in Tasikmalaya, West Java, Indonesia, with a coordinate coverage of 7°21'3.6''–7°14'58.92'' S and 108°6'12.24''–108°7'41.52''E, or UTM zone 49S. We re-process a total of 117 measurement points with an average measurement interval of approximately 600-700 meters using the recent gravity technique. The gravity survey was conducted using a LaCoste-Romberg type G gravimeter with an accuracy of 0.01 mGal. The height of the measurement points was determined using an altimeter with barograph correction.

The field survey data were corrected using standard gravity procedures, including tidal, drift, free-air, Bouguer, and terrain corrections, resulting in the Complete Bouguer Anomaly (CBA) (Blakely, 1996; Lowrie, 2007). The gravity measurements used a local base station tied to the absolute gravity benchmark DG0 in Bandung. The tidal correction was carried out using the well-known Longman equation, while the drift correction was calculated from the closed-loop base station measurements for each measuring day. The instrumental precision of the LaCoste-Romberg gravimeter is ±0.01 mGal. Considering repeat measurements at base stations, tidal corrections, and terrain corrections, the total uncertainty in CBA is estimated at ±0.15 mGal. The theoretical gravity at the reference ellipsoid was calculated using the 1980 International Gravity Formula. The average rock density of 2.57±0.05 g/cm^3 for the Bouguer correction was determined using the Parasnis method (1979). Local field corrections were performed through visual observation up to Zone D using the well-known Hammer chart.

The resulting Bouguer anomaly map, after various corrections, is shown in Figure 2a, along with regional Bouguer anomaly maps from the Geological Agency of Indonesia (Untung and Sato, 1978) (Figure 2b) and Martakusumah et al. (2015) (Figure 2c) for comparison. The three datasets show similar gravity anomaly patterns, with low anomalies in the centre flanked by high anomalies in the west and east, except for Martakusumah et al. (2015), whose data do not cover the eastern part of the study area. This indicates agreement of reading patterns among three different parties in the same area. The Bouguer anomaly value ranges differ slightly among the three; however, this is likely due to differences in several factors, including the latitude correction formula, elevation data, average density, and the terrain model used. The data in this study have a finer measurement interval than those of Martakusumah et al. (2015), which ranged from 1 to 2 km, thereby enabling higher lateral-resolution mapping of residual anomalies and subsurface structures and providing a more detailed view of the subsurface structure of the Galunggung area.

3.2 Regional-residual Anomaly Separation

Anomaly separation was performed to distinguish between the deeper and shallower depths. It is common practice to determine the cut-off value by observing the changes in the slope of the power spectrum curve as a function of wavenumber (Blakely, 1996; Buttkus, 2000). The separation of the regional and residual anomalies was performed using a Butterworth Band-pass Filter (BBF), preceded by spectral analysis to determine the spatial frequency cut-off values for band-pass filtering (e.g., Arisbaya et al., 2024). This method uses the Fourier transform to convert 2D spatial data to the frequency domain. In the frequency spectrum, anomalies with long wavelengths (low frequencies) are interpreted as originating from greater depths (regional), while those with short wavelengths (high frequencies) are from shallower depths (residual). On this basis, the regional anomalies are associated with deeper regional geological objects, while the residual anomalies are associated with shallower local objects.

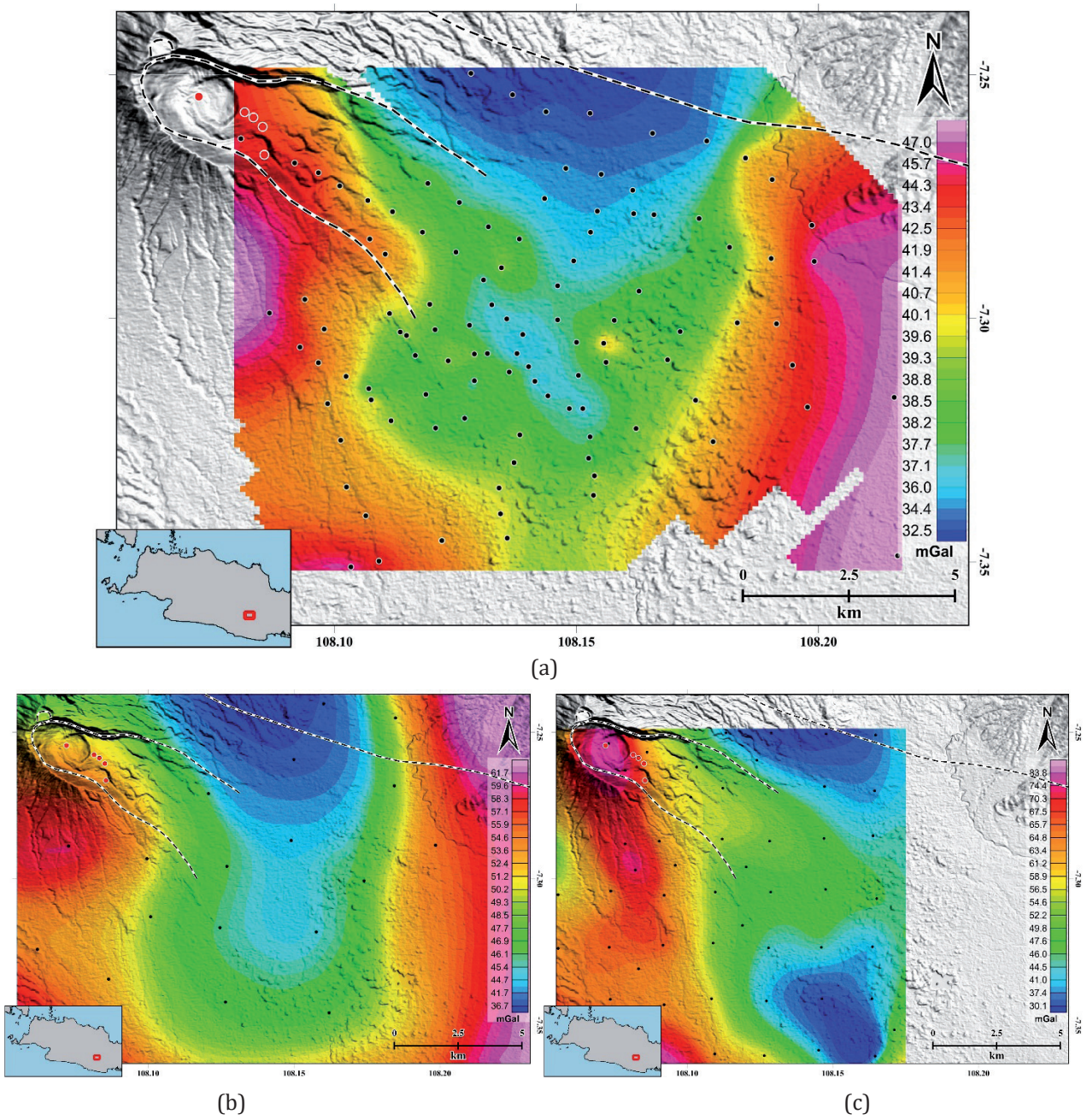

Figure 2. The Bouguer anomaly map of Galunggung and its surroundings, used in this study (a), is presented along with other Bouguer anomaly data from the Geological Agency (Untung and Sato, 1978)(b), and Martakusumah et al. (2015)(c) as a comparison. The black dots indicate gravity measuring stations, the black dashed line represents the structural interpretation as shown in Figure 1, while the red circles represent hot springs (Budhitrisna, 2010; Martakusumah et al., 2015).

Slope deflections in the radially averaged power spectrum occur at wavenumbers 0.30 and 0.90 cycle/km, dividing the curve into three frequency zones (low, middle, and high) (Figure 3). We applied a Butterworth Band-pass Filter with cut-off frequencies of 0.3–0.9 cycle/km to isolate residual anomalies, thereby eliminating low-frequency components associated with regional anomalies as well as the noise.

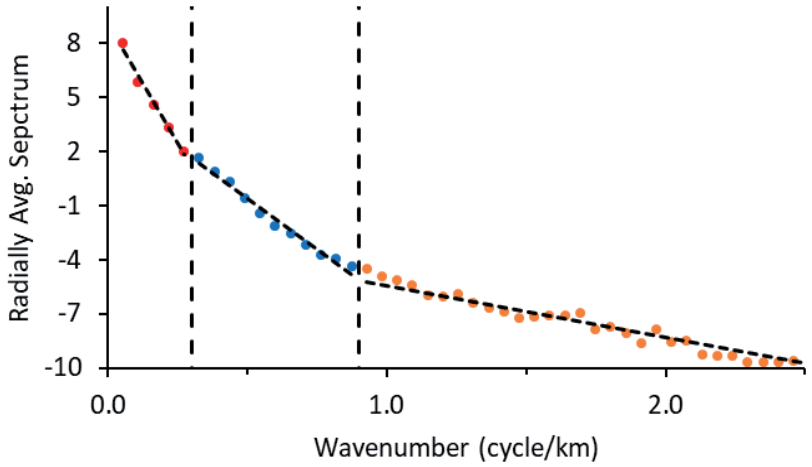

Figure 3. The spectral analysis of the gravity data aims to determine the spatial-frequency cut-off values for band-pass filtering.

For comparison, we also performed anomaly separation using a simple trend surface (TS) technique. In the TS technique, the regional trend of Bouguer anomalies is modeled by a polynomial curve. In the case of the Bouguer anomaly map $g_B(x, y)$, the polynomial can be written as follows (Lowrie, 2007):

$$g_B = g_0 + g_{x1}x + g_{y1}y + g_{x2}x^2 + g_{y2}y^2 + g_3x^3 + g_{y3}y^3 + \cdots + g_{xn}x^n + g_{yn}y^n$$

with *n* representing the order of the polynomial. TS uses a least-squares fitting of a low-order polynomial surface to estimate the regional components of the gravity field (Lowrie, 2007). Higher-order TS involves more polynomial terms, indicating more heterogeneous conditions or local variations associated with shallower depths. Since the regional Bouguer anomalies are linked to deeper regional geological features, the chosen TS order is the one that best represents the Bouguer anomalies, i.e., one with similar anomaly patterns. We performed 1st- to 3rd-order TS techniques; however, only the 3rd-order TS is shown here, as its regional anomaly closely matches the CBA map pattern.

3.3 Derivative Analysis

Derivative methods, such as vertical and horizontal gradients, are widely used to enhance the resolution of the gravity anomaly data interpretation. This approach is critical when Bouguer data exhibit subtle anomaly patterns, making it difficult to recognize the boundaries or geometry of subsurface structures. The first horizontal derivative (FHD) technique is the first derivative of the gravity anomaly in the lateral (x and y) directions. This analysis helps delineate the boundaries of geological bodies, such as faults, intrusions, and lithological variations. Meanwhile, the first vertical derivative (FVD) is the vertical derivative of the gravity anomaly g(x,y), which amplifies the response from sources near the surface. The magnitudes of the FHD and FVD were calculated using the following equations (Blakely, 1996):

$$FHD = \frac{\partial g}{\partial H} = \sqrt{\left(\frac{\partial g}{\partial x}\right)^2 + \left(\frac{\partial g}{\partial y}\right)^2}$$

$$FVD = \left(\frac{\partial g}{\partial z}\right) = \mathcal{F}\left(\frac{\partial g}{\partial z}\right)$$

where g is the Bouguer anomaly value. We applied a 3000 m cut-off wavelength low-pass filter to the Bouguer anomaly map before the derivative analysis.

In addition to FHD and FVD, we employed the normalized horizontal derivative (TDX), a geophysical data-processing method that enhances resolution and sharpens the contrast of subsurface structural anomalies. This technique was an improvement to tilt angle analysis (Miller and Singh, 1994). It is a normalized form of the total horizontal derivative, expressed mathematically as the ratio of the horizontal gradient amplitude to the vertical derivative of the gravity data (Cooper and Cowan, 2006).

$$TDX = tan^{-1}\left(\frac{HD}{|VD|}\right)$$

The use of ratios makes it insensitive to depth, unlike HD and VD, which show lower amplitudes for deeper objects when multiple objects at different depths are present. Meanwhile, expressing it in angular form (tan^{-1}) aims to limit its value within a fixed range, in this case, 0-90 degrees (Miller and Singh, 1994).

To validate our gravity-derived structural interpretation, we compared our results with: (1) surface geothermal manifestations mapped by Budhitrisna (2010), (2) structural lineaments from DEM analysis, and (3) crater morphology analysis by Marliyani et al. (2020).

4. Results and Discussion

The complete Bouguer anomaly (CBA) presented in Figure 2a, after various corrections, is influenced by differences in rock-mass distribution, resulting in a density contrast with the surrounding environment. Low-gravity anomalies (32.5–39.4 mGal) dominate the southeastern-central and northern parts of the study area. The low-gravity anomaly (blue-colored) in the north of the study area represents the confluence of products from three volcanoes: Galunggung, Talaga Bodas, and Ciremai. Although this area results from intense volcanic activity, the low anomaly indicates a more porous volcanic rocks (density ~2.2–2.4 g/cm^3), such as tuff and vesicular lava, compared to dense igneous basement (~2.7 g/cm^3). On the other hand, areas with high anomalies, particularly in the west and east, with a range of 40.1–48.1 mGal, indicate the presence of denser rocks, possibly massive igneous rocks or magma intrusions. According to Budhitrisna (2010), this area is a mixture of the old Galunggung product and other volcanoes, including Mt. Sawal, Mt. Kukus, Mt. Cakrabuana, and Mt. Sadakeling. The resulting products include volcanic breccia, flow breccia, tuff, lava, and lava with andesite-to-basalt compositions, which exhibit the characteristics of dense igneous rocks. In addition, these products include volcanic material that solidified beneath the surface, resulting in rocks with higher density than fragmented or porous materials.

The regional anomaly maps in Figure 4a (BBF) and Figure 4c (TS) are nearly identical to the CBA map (Figure 2a). Overall, the regional anomaly pattern indicates that the central and northern parts of the study area exhibit low anomalies, with values of approximately 32 and 39 mGal, respectively. In contrast, the western and northeastern parts exhibited strong anomalies (red to purple), with values ranging approximately from 39.6 to 48.2 mGal. Judging from the simpler pattern, we interpret that the TS regional anomalies were deeper than the BBF ones. Thus, the residuals from the BBF are estimated to depict a shallower subsurface than the results of the TS. The residual anomaly maps, Figure 4b and 4d range from -0.6 to 0.6 mGal. This relatively small range demonstrates the data's sensitivity to small-scale density variations arising from shallow layers, such as weathering and heterogeneities in lightweight volcanic materials. The residual anomaly maps, particularly the BBF, are dominated by a northwest-southeast trending pattern, which corresponds to the hot spring emergence pattern.

Faults are often identified by high FHD and zero FVD values at the same site (e.g., Hiramatsu et al., 2019; Wada et al., 2017). Figure 5 demonstrates that the low anomaly lineaments in the residual anomaly map have values greater than one mGal/km FHD (Figure 5a) and ~0 mGal/km FVD (Figure 5b), which can be interpreted as a fault. However, the lineament pattern is not as prominent as the features in the northwest and east areas. Thus, we implemented the TDX to elucidate the density contrasts. Derivative analysis reveals a relatively high TDX flanked by two low anomalies, suggesting that a NW-SE trending boundary follows the opening or breaching of Galunggung. The linear feature aligns with the hot springs on the slopes of Galunggung, following a southeastward-extending pattern. Two high TDX features with circular geometry are observed to the northeast (A1 and A2), yet no information was known on possible objects that might account for these circular features. The circular features A1 and A2 each result from single-point anomalies. While these could represent measurement noise amplified by derivative operations, they may also indicate small-scale intrusions or local density variations. Ground-truthing and additional measurements are needed to verify their origin.

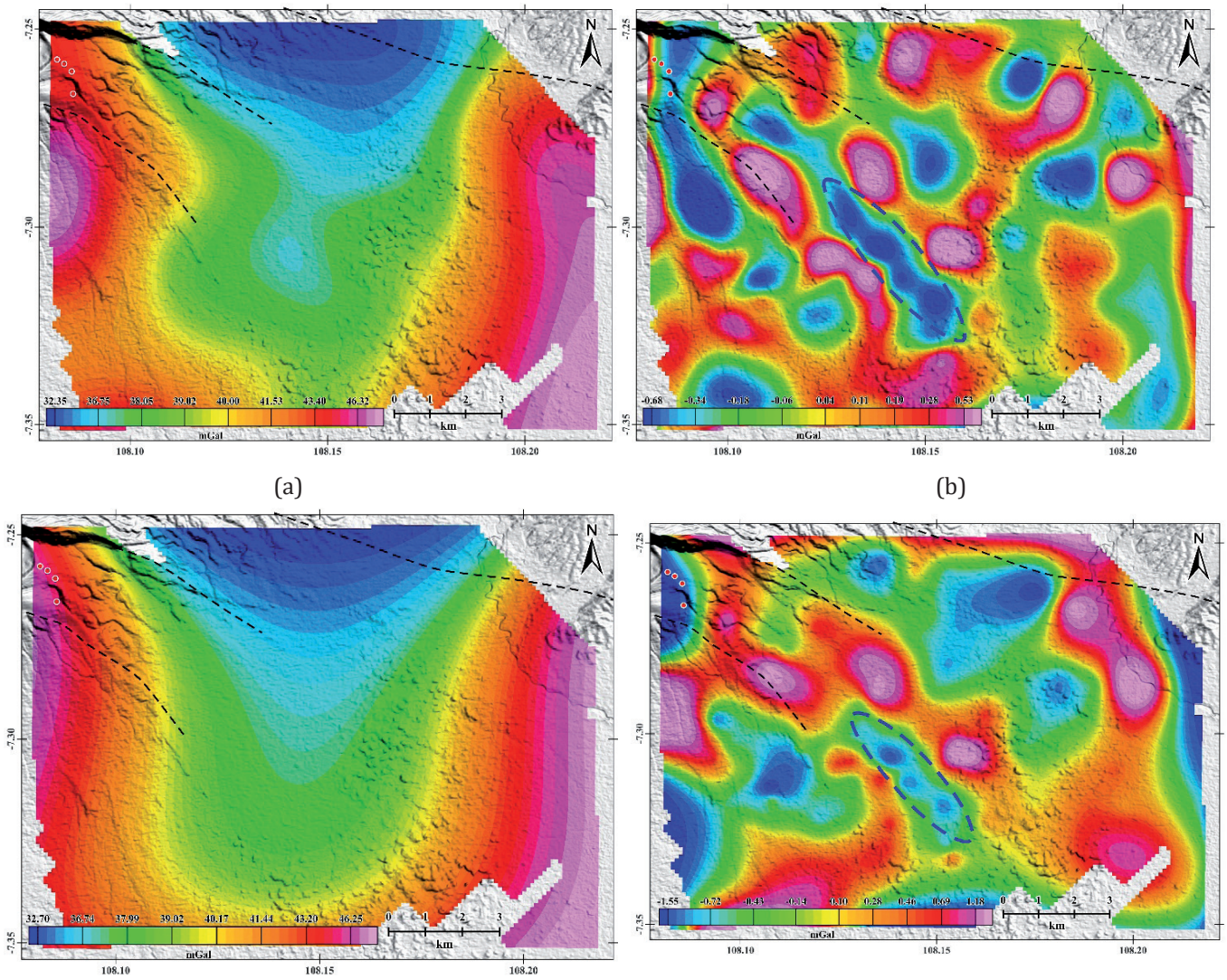

Figure 4. Regional gravity anomaly maps using BBF (a) and 3rd-order TS (c), as well as the residual anomaly maps using BBF (b) and 3rd-order TS (d). Dashed blue ellipse highlights a low-residual anomaly in the NNW-SSE direction in both BBF and TS modes, interpreted as a pre-existing fault.

Two additional high TDX features are also observed in the northwest and east areas (B1 and B2), both of which exhibit a curvy geometry. Based on the geological map and volcano history, the high-gravity anomaly in the western part of the regional map corresponds to rocks from the eruptions of Galunggung, both in the modern era and in the Old Galunggung Formation. Igneous rocks produced by volcanoes often have a tongue-like shape extending downward from the eruption center. During a stratovolcano build-up, multiple eruptions may result in a stack of tongue-shaped igneous rock bodies with tips varying in distance from the eruption's center, creating a curved shape geometry. Thus, based on their shape and location, we interpret the curvy, high TDX features as the boundaries of older volcanic products covered by younger volcanic products. In this case, the northwest and east curvy high TDX are interpreted as products of Old Galunggung and Mt. Sawal, respectively.

Multiple lines of evidence support a NW-SE trending subsurface fault: (1) linear low-gravity anomaly (C in Fig. 5c), (2) FHD>1 mGal/km with FVD~0 (fault signature), (3) alignment with hot spring distribution, (4) parallel to caldera opening morphology within the Galunggung breaching zone (C). Alternative interpretations for the NW-SE lineament include: (1) a volcanic rift zone, (2) lateral compositional variations, or (3) a buried paleovalley. However, these are less consistent with the alignment of geothermal manifestations and morphological evidence. Bronto (1989) stated that NW-SE striking faults were predominantly found in the Tertiary rocks of the study area, aligning with the lineaments of the young Galunggung cinder cone (1982-1983), which is perpendicular to the modern principal stress from the subduction zone. This study provides geophysical evidence for a NW-SE trending structure

parallel to the Galunggung opening. We propose a dual-role mechanism: (1) Pre-existing NW-SE fault served as a fluid pathway, causing hydrothermal alteration and rock weakening (Henley and Ellis, 1983), (2) Magma intrusion along this weak zone generated overpressure, triggering the fault-parallel sector collapse (Lagmay et al., 2000). However, numerical modeling is needed to quantify this process. Henley and Ellis (1983) suggested that hot springs, such as Cipanas and Citiis in the region, indicate geothermal activity related to faults or subsurface fractures, allowing hot fluids from deeper depths to rise through porous pathways or weak zones. The weak zone may also serve as a pathway for the volcanic vent to shift after the emplacement of the Old Galunggung, from the summit to the southeast flank, as suggested by Bronto (1989). In this sense, the structure is likely formed earlier and plays a dual role in the volcano's dynamics, serving as both a pathway for the migration of hot fluid and a structural weakness that facilitates collapse. Prolonged hydrothermal activity may lead to mineral weathering and reduced rock strength, resulting in unstable conditions. Magma intruding pre-existing faults can also activate these structures (Lagmay et al., 2000). The combination of rock weakening and pressure from magmatic activity could have created the conditions that triggered the volcanic avalanche. Figure 6 illustrates the fault-parallel breaching mechanism (adapted from Lagmay et al., 2000) that we propose to be responsible for the sector collapse of Galunggung and the resulting THT.

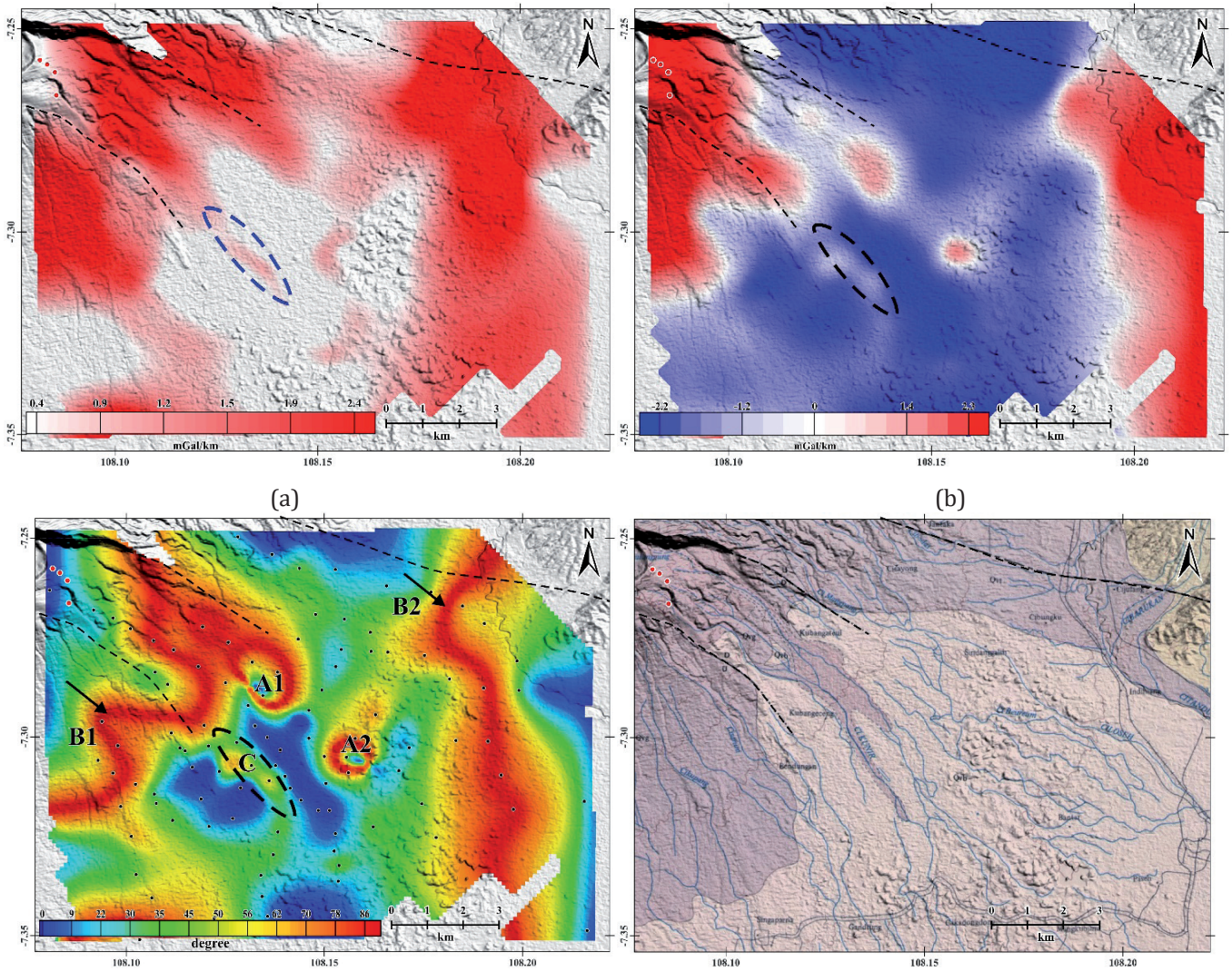

Figure 5. Map of the FHD (a), FVD (b), TDX (c), and surface geology (d) of the study area.

The collapse direction that is parallel to the fault strike is more often found in normal faults or strike-slip faults (Lagmay et al., 2000; Tibaldi, 1995). However, in this case, no active fault has been mapped in the region, and no cluster of tectonic seismicity has been reported. Thus, the possibility that the interpreted subsurface fault is active is less likely. Nevertheless, Alfin et al. (2022) reported a local normal fault with the N300E strike direction at one of their hummocky hills stop sites. Although they note that the fault does not appear to be connected

to any other major geologic lineaments, its presence in the active Quaternary volcanic area is noteworthy. This study suggests that pre-existing structural weaknesses played a crucial role in the collapse event. It is worth noting that certain geological processes may reactivate faults that have long been considered inactive.

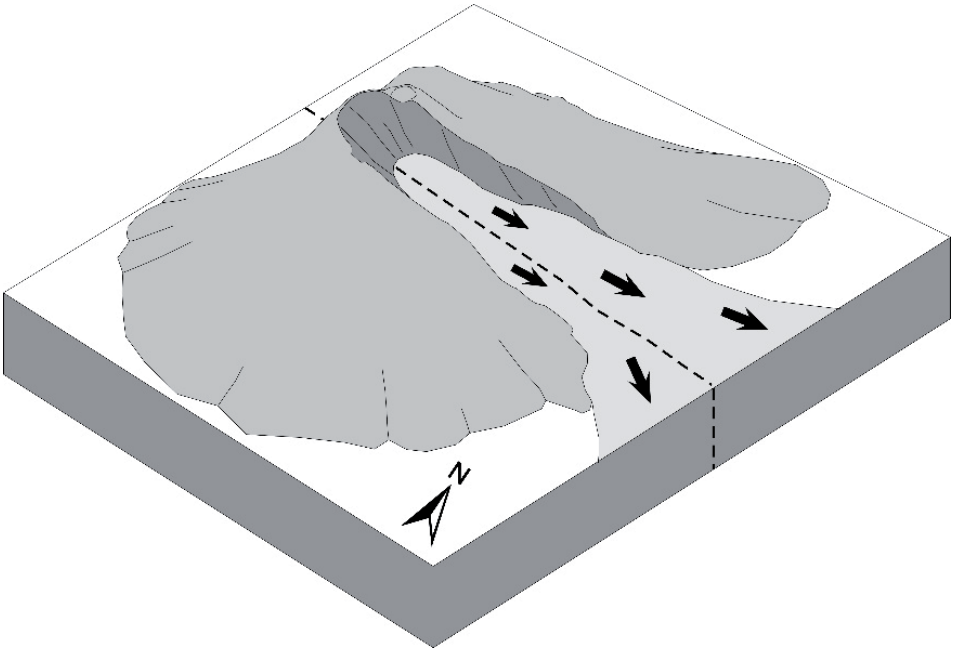

Figure 6. Illustration of proposed fault-parallel breaching (adapted from Lagmay et al., 2000) associated with the sector collapse of Galunggung.

Fault reactivation of inherited structures may occur through several mechanisms, including, but not limited to, plate tectonics reorganization (Kirby et al., 2007; Rimando and Peace, 2021), triggered by a major earthquake nearby (Farías et al., 2011; Husen and Kissling, 2001), magmatism and hydrothermal fluid (Arisbaya et al., 2023; Muluneh et al., 2021), or fluid injection into the reservoir (Chang and Segall, 2016; Passelègue et al., 2018). However, while this study provides geophysical evidence for a concealed fault that may be reactivated by various processes, the potential for earthquakes along this fault warrants a more comprehensive neotectonic investigation. Further investigation, such as detailed active fault mapping and paleoseismic analyses, is required to assess its potential to host an earthquake in the future.

5. Conclusions

We reprocessed 117 legacy gravity measurements and analyzed them using recent gravity techniques. The residual anomaly map shows a narrow low-gravity anomaly from the flank of the caldera extending in a NW-SE orientation, indicating a subsurface fault or fracture structure. The alignment of the geothermal manifestations on the southeastern flank slope supports this interpretation. Derivative analysis, including horizontal (FHD), vertical (FVD), and tilt (TDX) derivatives, revealed that the same NW-SE anomaly aligns with the opening or breaching zone. Furthermore, the TDX reveals a curvy geometry that, based on its shape and location, can be interpreted as old volcanic products covered by younger ones.

Gravity data analysis provides geophysical evidence for a NW-SE trending structure, parallel to and within the Galunggung breaching zone. This structure may play a dual role in the volcano's dynamics, serving as both a pathway for the migration of hot fluid and a structural weakness that facilitates collapse. After the emplacement of the Old Galunggung cryptodome, the volcanic conduit (and vent) shifted southeast along the weak zone. Prolonged hydrothermal activity in the weak zone may decrease the rock strength. The combination of rock weakening and pressure from magmatic activity could have triggered the volcanic avalanche along the inherited fault, resulting in the formation of the THT southeast of Galunggung. This suggests that pre-existing structures may act as weak zones that facilitate volcanic collapse, underscoring the importance of subsurface investigation for volcanic hazard mitigation.

Acknowledgments

We would like to express our gratitude to the editor and two anonymous reviewers for their feedback that significantly improved this paper. M. Dimas Ramadhana, R. Lucky Romadhon, and Sutan H. Firmansyah have also been invaluable for their insightful discussions. IA, MAM, and HG acknowledge support from the Riset Kolaborasi Indonesia (RKI) program 2025.

References

Al Kausar, A., Setiawan, I., Yuliyanti, A., Lintjewas, L., Jakah, Herawan, W., 2024. Geochemical characteristics of volcanic rocks in the Karaha–Talagabodas Field related to the Galunggung Volcano. J. Ris. Geol. dan Pertamb. 34, 25–40. https://doi.org/10.55981/risetgeotam.2024.1279

Alfin, A.S., Wibowo, H.E., Harijoko, A., 2022. Morphometric Characteristic and Distribution of Hummocky Hills in Debris Avalanche Deposit of Galunggung Volcano, West Java, Indonesia. IOP Conf. Ser. Earth Environ. Sci. 1071. https://doi.org/10.1088/1755-1315/1071/1/012012

Amir, H., Bijaksana, S., Dahrin, D., Nugraha, A.D., Arisbaya, I., Pratama, A., Suryanata, P.B., 2021. Subsurface structure of Sumani segment in the Great Sumatran Fault inferred from magnetic and gravity modeling. Tectonophysics 821. https://doi.org/10.1016/j.tecto.2021.229149

Arisbaya, I., Sudrajat, Y., Gaffar, E.Z., 2018. Model sistem panas bumi lapangan Karaha - Talaga Bodas berdasarkan inversi 2D data magnetotellurik. J. Ris. Geol. dan Pertamb. 28, 221–237. https://doi.org/10.14203/risetgeotam2018.v28.989

Arisbaya, I., Wijanarko, E., Sumintadireja, P., Warsa, W., Grandis, H., 2024. Deformation under a Young Volcanic Covered Area in Southern Garut, Indonesia: Insight from 3D Gravity Modelling. J. Math. Fundam. Sci. 55, 239–253. https://doi.org/10.5614/j.math.fund.sci.2024.55.3.3

Arisbaya, I., Wijanarko, E., Warsa, Sumintadireja, P., Sudrajat, Y., Handayani, L., Mukti, M.M., Grandis, H., 2023. Magnetotellurics (MT) and Gravity Study of a Possible Active Fault in Southern Garut, West Java, Indonesia. Int. J. Geophys. 2023. https://doi.org/10.1155/2023/4482074

Blakely, R.J., 1996. Potential Theory in Gravity and Magnetic, Cambridge University Press.

Bronto, S., 1989. Volcanic geology of Galunggung, West Java, Indonesia. University of Canterbury.

Budhitrisna, T., 2010. Geologic map of the Tasikmalaya quadrangle, West Java. Geological Research and Development Centre, Bandung.

Buttkus, B., 2000. Spectral Analysis and Filter Theory in Applied Geophysics. Springer Berlin, Heidelberg. https://doi.org/10.1007/978-3-642-57016-2

Chang, K.W., Segall, P., 2016. Injection-induced seismicity on basement faults including poroelastic stressing. J. Geophys. Res. Solid Earth 121, 2708–2726.

Cooper, G.R.J., Cowan, D.R., 2006. Enhancing potential field data using filters based on the local phase. Comput. Geosci. 32, 1585–1591. https://doi.org/10.1016/j.cageo.2006.02.016

Farías, M., Comte, D., Roecker, S., Carrizo, D., Pardo, M., 2011. Crustal extensional faulting triggered by the 2010 Chilean earthquake: The Pichilemu Seismic Sequence. Tectonics 30, 1–11. https://doi.org/10.1029/2011TC002888

Furuya, T., 1978. Preliminary Report on Some Volcanic Disasters in Indonesia. Japanese J. Southeast Asian Stud. 15, 591–597.

Henley, R.W., Ellis, A.J., 1983. Geothermal systems ancient and modern: a geochemical review. Earth Sci. Rev. 19, 1–50. https://doi.org/10.1016/0012-8252(83)90075-2

Hiramatsu, Y., Sawada, A., Kobayashi, W., Ishida, S., Hamada, M., 2019. Gravity gradient tensor analysis to an active fault: a case study at the Togi-gawa Nangan fault, Noto Peninsula, central Japan. Earth, Planets Sp. 71, 8. https://doi.org/10.1186/s40623-019-1088-5

Husen, S., Kissling, E., 2001. Postseismic fluid flow after the large subduction earthquake of Antofagasta, Chile. Geology 29, 847–850. https://doi.org/10.1130/0091-7613(2001)029<0847:PFFATL>2.0.CO;2

Kirby, S.M., Janecke, S.U., Dorsey, R.J., Housen, B.A., Langenheim, V.E., McDougall, K.A., Steeley, A.N., 2007. Pleistocene Brawley and Ocotillo Formations: Evidence for initial strike-slip deformation along the San Felipe and San Jacinto fault zonez, Southern California. J. Geol. 115, 43–62. https://doi.org/10.1086/509248

Lagmay, A.M.F., Vries, B. van W. de, Kerle, N., Pyle, D.M., 2000. Volcano instability induced by strike-slip faulting. Bull. Volcanol. 62, 331–346. https://doi.org/10.1007/s004450000103

Lowrie, W., 2007. Fundamentals of Geophysics, Second Edi. ed. Cambridge University Press, Cambridge.

Marliyani, G.I., Helmi, H., Arrowsmith, J.R., Clarke, A., 2020. Volcano morphology as an indicator of stress orientation in the Java Volcanic Arc, Indonesia. J. Volcanol. Geotherm. Res. 400, 106912. https://doi.org/10.1016/j.jvolgeores.2020.106912

Martakusumah, R., Srigutomo, W., Suryantini, N., Pratama, A.B., Haans, A., 2015. Gravity Analysis for Hidden Geothermal System in Cipanas, Tasikmalaya Regency, West Java, in: Proceedings World Geothermal Congress. Melbourne, pp. 19–25.

Miller, H.G., Singh, V., 1994. Potential field tilt — a new concept for location of potential field sources. J. Appl. Geophys. 32, 213–217. https://doi.org/10.1016/0148-9062(95)94633-0

Moore, J.N., Allis, R., Renner, J.L., Mildenhall, D., McCulloch, J., 2002. Petrologic evidence for boiling to dryness in the Karaha-Telaga Bodas geothermal system, Indonesia, in: Twenty-Seventh Workshop on Geothermal Reservoir Engineering. Stanford - California, p. 15.

Muluneh, A.A., Keir, D., Corti, G., 2021. Thermo-Rheological Properties of the Ethiopian Lithosphere and Evidence for Transient Fluid Induced Lower Crustal Seismicity Beneath the Ethiopian Rift. Front. Earth Sci. 9, 11. https://doi.org/10.3389/feart.2021.610165

Nemčok, M., Moore, J.N., Christensen, C., Allis, R.G., Powell, T., Murray, B., Nash, G., 2007. Controls on the Karaha – Telaga Bodas geothermal reservoir , Indonesia. Geothermics 36, 9–46. https://doi.org/10.1016/j.geothermics.2006.09.005

Nishida, J., Katsura, I., Nishimura, S., Jomori, A., Widarto, J.S., Arsadi, E.M., Nugroho, H.D., Gaffar, E.Z., Sudrajat, Y., 2001. Geophysical Survey of Guntur and Galunggung Volcanoes, West Java, Indonesia, in: Proceedings of the SEGJ Conference. The Society of Exploration Geophysicists of Japan, pp. 273–277.

Parasnis, D.S., 1979. Principles of Applied Geophysics, Third. ed. John Wiley & Sons, New York. https://doi.org/10.1007/978-94-009-5814-2

Passelègue, F.X., Brantut, N., Mitchell, T.M., 2018. Fault Reactivation by Fluid Injection: Controls From Stress State and Injection Rate. Geophys. Res. Lett. 45, 12,837-12,846. https://doi.org/10.1029/2018GL080470

Rimando, J.M., Peace, A.L., 2021. Reactivation Potential of Intraplate Faults in the Western Quebec Seismic Zone, Eastern Canada. Earth Sp. Sci. 8, 14. https://doi.org/10.1029/2021EA001825

Siebert, L., Roverato, Matteo, 2021. A Historical Perspective on Lateral Collapse and Volcanic Debris Avalanches, in: Roverato, M., Dufresne, A., Procter, J. (Eds.), Volcanic Debris Avalanches. Advances in Volcanology. Springer, Cham, pp. 11–50. https://doi.org/10.1007/978-3-030-57411-6_2

Suryo, I., Clarke, M.C.G., 1985. The occurrence and mitigation of volcanic hazards in Indonesia as exemplified at the Mount Merapi, Mount Kelut and Mount Galunggung volcanoes. Q. J. Eng. Geol. Hydrogeol. 18, 79–98. https://doi.org/10.1144/gsl.qjeg.1985.018.01.09

Tibaldi, A., 1995. Morphology of pyroclastic cones and tectonics. J. Geophys. Res. 100, 24521–24535.

Untung, M., Sato, Y., 1978. Gravity and geological studies in Java, Indonesia, Special Publication. Geological Survey of Indonesia and Geological Survey of Japan.

Wada, S., Sawada, A., Hiramatsu, Y., Matsumoto, N., Okada, S., 2017. Continuity of subsurface fault structure revealed by gravity anomaly: the eastern boundary fault zone of the Niigata plain, central Japan. Earth, Planets Sp. 69, 12. https://doi.org/10.1186/s40623-017-0602-x

Wu, Y., Gao, Y., 2019. Gravity pattern in southeast margin of Tibetan Plateau and its implications to tectonics and large earthquakes. Earth Planet. Phys. 3, 425–434. https://doi.org/10.26464/epp2019044